ISSN 0021-8944, Journal of Applied Mechanics and Technical Physics, 2014, Vol. 55, No. 6, pp. 1055–1065. © Pleiades Publishing, Ltd., 2014.
Original Russian Text © V.D. Kurguzov, N.S. Astapov, I.S. Astapov.

FRACTURE MODEL FOR STRUCTURED QUASIBRITTLE MATERIALS

V. D. Kurguzov[a], N. S. Astapov[a], and I. S. Astapov[b]

UDC 539.3

Abstract: We analyze the applicability of a modified Leonov–Panasyuk–Dugdale model to the description of the propagation of a mode I crack in structured materials under plane stress conditions. For quasi-brittle materials, refined formulas of the critical length of the prefracture zone and the critical load containing a structural parameter are proposed. The Kornev model is extended to the case of quasi-ductile materials. Numerical simulation of plastic zones in square plates of a bimetal and a homogeneous material under quasi-static loading is performed. In the numerical model, the equations of deformable solid mechanics are expressed in the Lagrangian formulation, which is the most preferred for large-strain deformations of elastoplastic materials. The results of the numerical experiments are consistent with the results of calculations using the analytical model for the fracture of structured materials.

Keywords: fracture criteria, prefracture zone, characteristic size of structural element, quasi-ductile fracture diagram.

DOI: 10.1134/S0021894414060182

INTRODUCTION

In a review of experimental studies [1], it is noted that one of the most important factors causing fracture in engineering structures is the presence of hidden cracks or crack-like defects. In addition, problems in constructing analytical fracture models within the framework of linear fracture mechanics (LFM) are considered, especially for structures of complex geometry under creep conditions. In [2], atomistic notions of solid state physics and dislocation theory were used to describe the plastic zone. As a result, in the plastic zone, a semicircle (core) with center at the tip of a real crack was distinguished within which the LFM approach is inapplicable. The dependence of the characteristics of this core on the physical parameters of the materials, including the work of adhesion were studied numerically. Since many of the parameters used in [2] are difficult to evaluate or are estimated heuristically, the approach proposed in that paper allows only a qualitative description of the fracture mechanism.

Solutions of problems of cracks in bodies of finite sizes are of practical interest, but for such cases there are no solutions in closed form. These problems are complex due to the boundary conditions [3]. It has been shown [4] that the fracture criteria considering the characteristic size of the material structure has an extended range of application compared to the traditional criteria, although the issue of how this size is related to the composition, structure, and possibly other parameters of real materials has not been studied. The fracture model presented below is partially described in [5], but, in this paper, too, there are no finite simple formula suitable for engineering calculations. Problems the closest to the one considered in the present paper are studied in [6], where the fracture process is described taking into account the elastic limits of the composite constituent materials, but not their structure.

[a]Lavrent'ev Institute of Hydrodynamics, Siberian Branch, Russian Academy of Sciences, Novosibirsk, 630090 Russia; kurguzov@hydro.nsc.ru; nika@hydro.nsc.ru. [b]Research Institute of Mechanics, Lomonosov Moscow State University, Moscow, 119192 Russia; velais@imec.msu.ru. Translated from Prikladnaya Mekhanika i Tekhnicheskaya Fizika, Vol. 55, No. 6, pp. 173–185, November–December, 2014. Original article submitted August 27, 2013; revision submitted January 27, 2014.

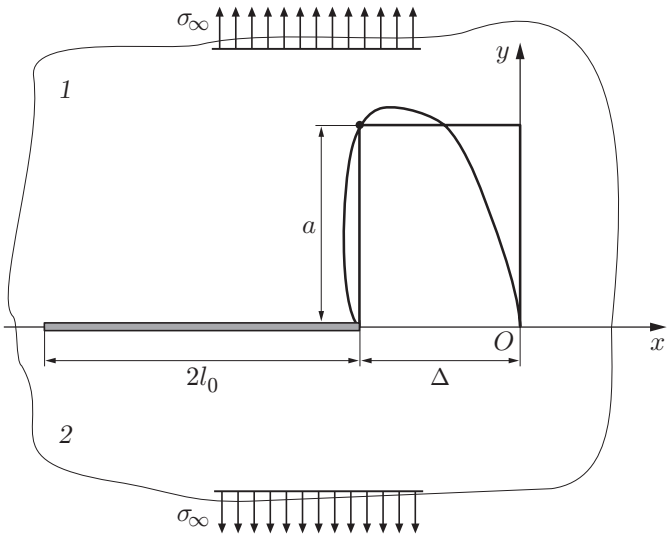

Fig. 1. Approximation of the plastic zone at the crack tip located at the interface: (*1*) material 1; (*2*) material 2.

In the present paper, the fracture of structured materials is described using a modified Leonov–Panasyuk–Dugdale model of the prefracture zone with necessary and sufficient failure criteria (Neuber–Novozhilov approach). A modification of this analytical model was performed by Kornev [7, 8] and is used to solve various problems of quasi-brittle fracture, so that it will be called the Kornev model. The main feature that distinguishes the Kornev model from the classical Leonov–Panasyuk–Dugdale model is the presence of the width of the prefracture zone—an additional parameter that models the diameter of the plastic zone. The introduction of this parameter allows a more accurate evaluation of the destruction of the structure of the prefracture zone using information on the parameters of the standard ($\sigma-\varepsilon$) diagrams of materials (σ is the stress and ε is the strain). This work is a continuation of [9–12]. The basic assumptions of the Kornev model for a mode I crack located in the center of a structured bimetallic square plate of size $L \times L$ along a straight-line interface are given below [9, 11]. The approximate relations of the Kornev model are refined. The results of calculations using the refined model are compared with the results of numerical experiments for cracks in a bimetallic plate [10] and a homogeneous structured plate [12].

1. KORNEV MODEL

We consider a square bimetallic plate of size $L \times L$ with a central internal crack of length $2l_0$, subjected to axial tension by stresses σ_∞ defined at the edges. Suppose that $E_1 = E_2$ and $\mu_1 = \mu_2$, where E_1, μ_1 and E_2, μ_2 are the Young's modulus and Poisson's ratios of materials 1 and 2, respectively. Let the materials of the upper and lower parts of the plate differ only beyond the yield points: $\sigma_{Y1} < \sigma_{Y2}$. We introduce a coordinate system Oxy in the plane of the square plate [7–10]. The coordinate origin coincides with the tip of the fictitious crack and the tip of the real crack has the abscissa $x = -\Delta$ (Fig. 1). The ordinate Oy is perpendicular to the plane in which the crack propagates.

In constructing fracture diagrams and a rectangular prefracture zone of size $\Delta \times a$ ahead of the crack tip in the bimetal, we use the sufficient fracture criteria (Neuber–Novozhilov approach)

$$\frac{1}{kr_1}\int\limits_0^{nr_1} \sigma_y(x,0)\,dx \leqslant \sigma_{Y1}, \qquad x \geqslant 0; \tag{1}$$

$$2\nu(x) \leqslant \delta_1^*, \qquad -\Delta \leqslant x < 0. \tag{2}$$

Here $\sigma_y(x,0)$ is the normal stress on the crack continuation, n and k are natural numbers ($1 \leqslant k \leqslant n \leqslant 4$), nr_1 is the averaging interval, r_1 is the characteristic linear size of the structural element of material 1, the function $\nu = \nu(x)$ is

the crack half-opening, $\delta_1^* = (\varepsilon_{11} - \varepsilon_{01})a$ is the critical opening of the crack model for the homogeneous material, ε_{01} is the maximum elastic elongation, and ε_{11} is the maximum relative elongation of the less strong ($\sigma_{Y1} < \sigma_{Y2}$) material 1.

The diameter a of the prefracture zone is identified with the half-diameter (only one, the less strong metal is under plasticity conditions) of the plastic zone [9, 13] at the tip of the real crack in the homogeneous material:

$$a = 5(K_{\mathrm{I}\infty}/\sigma_{Y1})^2/(8\pi). \tag{3}$$

At $x = -\Delta$, inequality (2) becomes the equality [11]

$$\frac{8\varepsilon_{01}}{\sigma_{Y1}}\,(K_{\mathrm{I}\infty} + K_{\mathrm{I}\Delta})\sqrt{\frac{\Delta}{2\pi}} = (\varepsilon_{11} - \varepsilon_{01})\,\frac{5Y^2}{8\pi}\Big(\frac{\sigma_\infty}{\sigma_{Y1}}\Big)^2 l, \tag{4}$$

where $2l = 2l_0 + 2\Delta$ is the length of the model crack. In equality (4), the stress intensity factor (SIF) $K_{\mathrm{I}\infty}$ due to the stress σ_∞ will be represented by the following approximating formula [3, p. 74] for a central crack, which takes account the finite dimensions of the sample:

$$K_{\mathrm{I}\infty} = Y\sigma_\infty\sqrt{l},$$

where $Y = \sqrt{\pi/\cos(\pi l/L)}$, and the SIF due to the constant stress σ_{Y1} acting in accordance to the Leonov–Panasyuk–Dugdale model by the formula

$$K_{\mathrm{I}\Delta} = -\sigma_{Y1}\sqrt{\pi l}\,[1 - 2\arcsin(1 - \Delta/l)/\pi]. \tag{5}$$

Simplifying expressions (5) by using the approximation

$$\arcsin(1 - \Delta/l) \approx \pi/2 - \sqrt{2\Delta/l}, \tag{6}$$

we obtain $K_{\mathrm{I}\Delta} \approx -2\sigma_{Y1}\sqrt{2\Delta/\pi}$. Equation (4) can be written in the form of a quadratic equation with respect to $\sqrt{\Delta/l}$:

$$\frac{8\varepsilon_{01}}{\sigma_{Y1}}\Big(\frac{Y\sigma_\infty}{\sqrt{2\pi}} - \frac{2\sigma_{Y1}}{\pi}\sqrt{\frac{\Delta}{l}}\Big)\sqrt{\frac{\Delta}{l}} = (\varepsilon_{11} - \varepsilon_{01})\,\frac{5}{8}\Big(\frac{Y\sigma_\infty}{\sqrt{\pi}\sigma_{Y1}}\Big)^2. \tag{7}$$

Discarding the small term containing Δ/l in relation (7), we obtain an approximate expression corresponding to the smallest root for the critical length of the prefracture zone in the less strong material:

$$\Delta = 25\Big(\frac{\varepsilon_{11} - \varepsilon_{01}}{\varepsilon_{01}}\Big)^2\Big(\frac{Y\sigma_\infty}{\sigma_{Y1}}\Big)^2\frac{l}{2^{11}\pi}. \tag{8}$$

For the critical values of σ_∞ and Δ, inequality (1) also becomes an equality. Substituting into (1) the approximate representation of the normal stresses $\sigma_y(x, 0)$ on the continuation of the central crack in a sample of finite size [11, 14]:

$$\sigma_y(x, 0) = \frac{K_{\mathrm{I}\infty}}{\sqrt{2\pi x}} + \frac{L}{L - 2l}\,\sigma_\infty + \frac{K_{\mathrm{I}\Delta}}{\sqrt{2\pi x}}, \qquad x \geqslant 0, \tag{9}$$

and integrating, we have the equality

$$(K_{\mathrm{I}\infty} + K_{\mathrm{I}\Delta})\sqrt{\frac{2nr_1}{\pi}} + \frac{L}{L - 2l}\,\sigma_\infty nr_1 = \sigma_{Y1}kr_1. \tag{10}$$

In (10), we also substitute the approximation (6) for the expression $K_{\mathrm{I}\Delta} \approx -2\sigma_{Y1}\sqrt{2\Delta/\pi}$, from which Δ is eliminate using representation (8). Finally, for the critical stress σ_∞, we obtain the relation

$$\frac{\sigma_\infty}{\sigma_{Y1}} = \frac{1}{Y}\Big[\sqrt{\frac{2l}{\pi r_1}}\,\frac{n}{k^2}\Big(1 - \frac{5}{16\pi}\,\frac{\varepsilon_{11} - \varepsilon_{01}}{\varepsilon_{01}}\Big) + \frac{L}{L - 2l}\,\frac{1}{Y}\,\frac{n}{k}\Big]^{-1}. \tag{11}$$

Formulas (8) and (11) describe the critical length of the prefracture zone Δ and the critical fracture stress σ_∞ in the case where the crack is located along the interface and the approximate representation of the normal stress $\sigma_y(x, 0)$ on the continuation of the crack is chosen in the form (9).

We introduce the dimensionless critical stress $\lambda = \sigma_\infty/\sigma_{Y1}$ (the critical stress referred to the yield point) and the parameter $\chi = (\varepsilon_{11} - \varepsilon_{01})/\varepsilon_{01}$, which can be called the plasticity index or the reciprocal of the brittleness index. Then, after a series of transformations, formulas (8) and (11) can be written as

$$\Delta = 25\chi^2\lambda^2 lY^2/(2^{11}\pi); \tag{12}$$

$$\lambda = \frac{k}{n}\Big[\frac{Y}{\sqrt{\pi}}\sqrt{\frac{2l}{nr_1}}\Big(1 - \frac{5\chi}{16\pi}\Big) + \frac{L}{L - 2l}\Big]^{-1}. \tag{13}$$

Formula (13), which is more compact than (11), allows a better representation of the results of calculations using the proposed model.

2. REFINED KORNEV MODEL

Let us analyze the obtained system of formulas (12) and (13). System (1) and (2) is equivalent to system (4), (10) written using the SIF, provided that both systems contain the same function $\sigma_y(x,0)$ of the normal stress on the crack continuation and the same function of the crack half-opening $\nu = \nu(x)$. In Eqs. (4) and (10), the coefficient $K_{\mathrm{I}\Delta}$ is represented using approximation (6). This approximation is valid due to the inequality $\Delta/l \ll 1$. Indeed, the error of approximation (6) does not exceed 0.4% at $0 \leqslant x \leqslant 0.1$ ($x = \Delta/l$) and does not exceed 6% as x increases to the value $x \approx 0.4288$. In addition, when solving Eqs. (7), the term containing Δ/l is dropped. Thus, in solving the basic equation (4), we the coefficient $K_{\mathrm{I}\Delta}$ describing the prefracture zone is neglected (set to zero). The real roots of Eq. (7)

$$\Delta_{+,-} = \pi Y^2\lambda^2 l\Big(1 \pm \sqrt{1 - 5\chi/(4\pi)}\Big)^2 \Big/ 32 \tag{14}$$

exist only if $\chi \leqslant 4\pi/5 \approx 2.5$. At $\chi \ll 2.5$, for the smaller root Δ_- with two terms of the binomial expansion taken into account, we obtain the approximate equality $\Delta_- \approx \pi Y^2\lambda^2 l(5\chi/(8\pi))^2/32 = 25\chi^2\lambda^2 l Y^2/(2^{11}\pi)$, which coincides with expressions (8) and (12). Therefore, the approximation (8) applies only if $\chi \ll 2.5$. Note that this restriction is significantly stronger than the restriction $\chi \leqslant 16\pi/5 \approx 10$ implied by formula (11) of the Kornev model for $n = k = 1$ [9–11].

We refine the expression for the critical length Δ of the prefracture zone without using approximation (6) in relation (5). For this, we rewrite system (4), (10) as follows:

$$\frac{K_{\mathrm{I}\infty} + K_{\mathrm{I}\Delta}}{\sigma_{Y1}} = \Big(\frac{k}{n} - \frac{L\lambda}{L - 2l}\Big)\sqrt{\frac{\pi n r_1}{2}}\,; \tag{15}$$

$$\frac{K_{\mathrm{I}\infty} + K_{\mathrm{I}\Delta}}{\sigma_{Y1}}\sqrt{\frac{\Delta}{2\pi}} = \frac{\chi c Y^2\lambda^2 l}{8\pi}. \tag{16}$$

Here $c = 5/8$ in the case of plane stress. In Eq. (16), we substitute the expression $K_{\mathrm{I}\infty} + K_{\mathrm{I}\Delta}$ from Eq. (15) and in Eq. (15), the relation $K_{\mathrm{I}\infty} = Y\sigma_\infty\sqrt{l}$ and relation (5) for the coefficient $K_{\mathrm{I}\Delta}$. As a result, we obtain a system of equations equivalent to the system of equations (15) and (16), and consequently, to the basic system of equations (1) and (2):

$$\frac{\lambda Y}{\sqrt{\pi}} - \Big[1 - \frac{2}{\pi}\arcsin\Big(1 - \frac{\Delta}{l}\Big)\Big] = \Big(\frac{k}{n} - \frac{L\lambda}{L - 2l}\Big)\sqrt{\frac{n r_1}{2l}}\,; \tag{17}$$

$$\Big(\frac{k}{n} - \frac{L\lambda}{L - 2l}\Big)\sqrt{\frac{\pi n r_1}{2}}\sqrt{\frac{\Delta}{2\pi}} = \frac{\chi c Y^2\lambda^2 l}{8\pi}. \tag{18}$$

System (17), (18) will be called exact. From Eq. (18), assuming that the expression in brackets is not zero ($K_{\mathrm{I}\infty} + K_{\mathrm{I}\Delta} \neq 0$), we obtain an exact expression for the length of the prefracture zone in a bimaterial sample of finite size:

$$\sqrt{\Delta} = \frac{\chi c Y^2\lambda^2 l}{4\pi}\Big[\Big(\frac{k}{n} - \frac{L\lambda}{L - 2l}\Big)\sqrt{n r_1}\Big]^{-1},$$

which for $c = 5/8$ can be written in a form convenient for comparison with formula (12):

$$\Delta = \frac{25\chi^2\lambda^2 Y^4}{2^{11}\pi^2}\,\frac{2l^2}{n r_1}\Big(\frac{k}{n\lambda} - \frac{L}{L - 2l}\Big)^{-2}. \tag{19}$$

Note that in contrast to formula (12), expression (19) for the length of the prefracture zone depends explicitly (not implicitly through λ) on the parameters k and n characterizing the damage to the starting material, and also depends on the characteristic size r_1 of the structural element of the material. Expression (19) is exact as it is derived from Eqs. (4) and (10) for $K_{\mathrm{I}\infty} = Y\sigma_\infty\sqrt{l}$ without using any approximation for the coefficient $K_{\mathrm{I}\Delta}$.

Lengths Δ and r_1 for different critical loads λ

λ	FEM	Basic model		Refined model			
	Δ_E, mm	Δ_K, mm	r_{1K}, mm	Δ_M, mm	r_{1M}, mm	Δ_P, mm	r_{1P}, mm
0.0680	0.040	0.000 44	0.166	0.000 52	0.164	0.083	0.0010
0.0752	0.060	0.000 54	0.208	0.000 63	0.205	0.101	0.0013
0.0821	0.081	0.000 65	0.253	0.000 75	0.250	0.120	0.0016
0.0889	0.102	0.000 76	0.303	0.000 88	0.300	0.141	0.0019
0.1026	0.146	0.001 01	0.423	0.001 18	0.418	0.188	0.0026
0.1163	0.204	0.001 30	0.569	0.001 51	0.562	0.241	0.0035
0.1436	0.356	0.001 98	0.955	0.002 30	0.944	0.368	0.0059
0.1710	0.543	0.002 80	1.498	0.003 26	1.480	0.522	0.0093
0.2326	1.219	0.005 19	3.550	0.006 04	3.509	0.965	0.0220
0.3352	3.902	0.010 80	12.100	0.012 50	11.960	2.004	0.0749

Using approximation (6) in Eq. (17) and taking into account equality (18), we obtain a quadratic equation with respect to λ:

$$\Big(\Big(\frac{L}{L-2l}\Big)^2\sqrt{\frac{\pi n r_1}{2l}}+\frac{LY}{L-2l}+\sqrt{\frac{2l}{\pi n r_1}}\,\frac{\chi c Y^2}{2\pi}\Big)\lambda^2-\frac{k}{n}\Big(Y+\frac{2L}{L-2l}\sqrt{\frac{\pi n r_1}{2l}}\,\Big)\lambda+\frac{k^2}{n^2}\sqrt{\frac{\pi n r_1}{2l}}\approx 0. \tag{20}$$

System (18), (20) will be called approximate. The roots of Eq. (20) can be written as follows:

$$\lambda_{+,-}\approx\frac{k}{2n}\Big(\frac{2L}{L-2l}+\frac{Y}{\sqrt{\pi}}\sqrt{\frac{2l}{nr_1}}\Big(1\pm\sqrt{1-\frac{2\chi c}{\pi}}\,\Big)\Big)\Big/\Big(\frac{L^2}{(L-2l)^2}+\frac{LY}{L-2l}\sqrt{\frac{2l}{\pi n r_1}}+\frac{\chi c Y^2 l}{\pi^2 n r_1}\Big). \tag{21}$$

Note that in the case of plane stress ($c=5/8$), the real roots of $\lambda_{+,-}$ of Eq. (21), as well as the roots of Eq. (14), exist only for $\chi\leqslant 4\pi/5\approx 2.5$ and they are nonnegative.

3. COMPARISON OF THE RESULTS OF ANALYTICAL AND NUMERICAL CALCULATIONS

Formulas (12) and (13) of the Kornev model and formulas (19) and (21) of the refined model allow calculating the length Δ of the prefracture zone and the characteristic linear size r_1 of the structural element of the material from the value of the critical load λ. Let us compare the results of calculations using these formulas and the numerical simulation results.

3.1. Length of the Prefracture Zone in Bimetal

In [10], a $100.0\times 100.0\times 0.4$ mm bimetallic square plate with a central crack of length $2l_0=30$ mm in a plane stress state under tensile stress σ_∞ applied to the edge was considered. The plate materials had the following characteristics: $E_1=E_2=2\cdot 10^5$ MPa, $\mu_1=\mu_2=0.25$, $\sigma_{Y1}=340$ MPa, and $\sigma_{Y2}=500$ MPa. Paper [10] presents the results obtained by a finite element method (FEM) with a numerical simulation of the real form of the plastic zone in the vicinity of the tip of a mode I crack propagating along the interface between two metals. The values of the critical fracture load λ and the length of the corresponding pre-fracture zone Δ_E calculated using the FEM [10] ate shown in the table.

Let us compare the values of Δ_E obtained in the numerical experiment with the results of predicting the length Δ of the prefracture zone at a given load λ using the analytical model. In addition to the parameters σ_∞, σ_{Y1}, and Δ, the exact formulas (4) and (10) contain the unknown mechanical characteristic of the material χ and the unknown geometric parameters r_1 and l of the structure. Calculations using the Kornev model [10] for the given values of $n=k=1$ and $l=15$ mm have shown that the parameters χ and r_1 vary with the load λ. If the characteristic linear size r_1 of the structural element of the material is assumed to be constant, then, as the critical load λ increases by a factor of five (see [10, Table 1]), the plasticity index χ increases by a factor of three, and vice versa, for a fixed value of χ, the value of r_1 varies with the load. Apparently, this dependence is due to the influence of the interfacial layer in regions close to the interface in the composite. The possibility of increasing the tensile strength of the material by physicochemical interactions between the phases is discussed in detail in [15].

Recall that the equations of continuum mechanics used in FEM numerical simulations do not contain the parameter r_1 [12]; therefore, we compare the results in the following manner. Assume that for a composite composed of the materials used in [10], there are values of χ and r_1 that are the same for all the load values λ given in the table. Let $l = 15$ mm. Then, for a fixed load λ_1, the system of exact equations (17) and (18) for $n = k = 1$ contains three unknown quantities: Δ_1, χ, and r_1, and the last two unknowns have the same values for any load λ_2 to which a certain value of the length of the prefracture zone Δ_2 corresponds.

We compose a system of four equations with four unknowns χ, r_1, Δ_1, and Δ_2 corresponding to two different load values λ_1 and λ_2, and find its solution numerically. For $\lambda_1 = 0.048$ and $\lambda_2 = 0.3352$, we obtain $\chi \approx 0.683$, $r_1 \approx 0.0768$, $\Delta_1 \approx 0.00026$, and $\Delta_2 \approx 1.956$. Setting $\chi = 0.683$, we calculate the values of Δ and r_1 for each value of the load in the table by solving the system of exact equations (17) and (18). The calculations show that there are two different solutions: Δ_M, r_{1M} and Δ_P, r_{1P} (see the table). The values of Δ_M are in poor agreement with the values of Δ_E obtained by the numerical simulation: Δ_M is 80–300 times smaller than Δ_E. In contrast, the values of Δ_P are in satisfactory agreement with the values of Δ_E. In addition, we note that the values of Δ_P vary in the range $26r_{1P}$–$86r_{1P}$. The table also shows the values of the prefracture zone length Δ_K calculated by formula (12) of the Kornev model, which, for all the load values considered, approximate the values of Δ_M fairly well; $\Delta_K < \Delta_M$. The values of the characteristic linear size r_{1K} of the structural element of the material in the Kornev model listed in the table were calculated from a predetermined load using equality (13). To elucidate the effect of approximation (6) on the accuracy of the calculations for each load value by formula (14) we determined the roots of the quadratic equation (7). It was found that for all load values $\lambda \leqslant 0.1436$, the roots $\Delta_{+,-}$ of Eq. (7) coincide, up to three significant figures, with the values of Δ_P and Δ_M given in the table and with the solutions of the approximate system (18), (20).The results of the calculations also show that for a given load λ, the plus sign in formula (21) corresponds to the value of r_{1P} in the table, and the minus sign to the value of r_{1M}.

Thus, from the analysis of the data in the table, it can be concluded that it is the value of λ_- calculated by formula (21) that is the critical load for quasi-brittle fracture. For $\chi = 0$ (brittle fracture), we have the equality $\lambda_- \approx k/(L/(L-2l) + Y\sqrt{2l/(nr_1)}\,/\sqrt{\pi}\,)/n$, which coincides with the expression obtained by formula (13) of the Kornev model in the case of brittle fracture.

However, it was shown in [12] that in a numerical simulation of a bimetallic square plate having the same characteristics as the plate studied in this paper and in [10] of the plate, quasi-brittle fracture was considered. The results of numerical simulation given in [10] (values of Δ_E in the table) agree much better with the results of calculations by formula (21) in the case of λ_+ (values of Δ_P in the table). Consequently, formula (21) in the case λ_+ describes quasi-ductile fracture. Additional arguments for this statement are given below.

3.2. Fracture Diagrams for Bimaterial

In the Kornev model [9, 10], the normal stresses $\sigma_y(x, 0)$ on the crack continuation are approximately represented by the following [different from (9)] expression

$$\sigma_y(x,0) \approx \frac{\sigma_\infty |x+l|}{\sqrt{(x+l)^2 - l^2}} + \frac{K_{\mathrm{I}\Delta}}{\sqrt{2\pi x}}, \qquad K_{\mathrm{I}\infty} = \sigma_\infty \sqrt{\pi l}, \tag{22}$$

which does not take into account the finite dimensions of the plate. In this case, the critical length Δ of the prefracture zone in the less strong materials and the dimensionless critical stress λ are expressed in [10] as follows:

$$\Delta = 25\chi^2\lambda^2 l/2^{11}; \tag{23}$$

$$\lambda = \frac{k}{n}\Big(\sqrt{1 + \frac{2l}{nr_1}} - \frac{5\chi}{16\pi}\sqrt{\frac{2l}{nr_1}}\,\Big)^{-1}. \tag{24}$$

Note that if the function $\sigma_y(x, 0)$ is chosen in the form (22), the length Δ in expression (23) of the Kornev model does not depend explicitly on the parameters k, n, and r_1, as in Eq. (12). In the refined model with the function $\sigma_y(x, 0)$ in the form (22), the constitutive equations equivalent to system (1), (2) and similar to relations (17) and (18) are written as

$$\lambda\sqrt{1 + \frac{nr_1}{2l}} - \frac{k}{n}\sqrt{\frac{nr_1}{2l}} = 1 - \frac{2}{\pi}\arcsin\Big(1 - \frac{\Delta}{l}\Big); \tag{25}$$

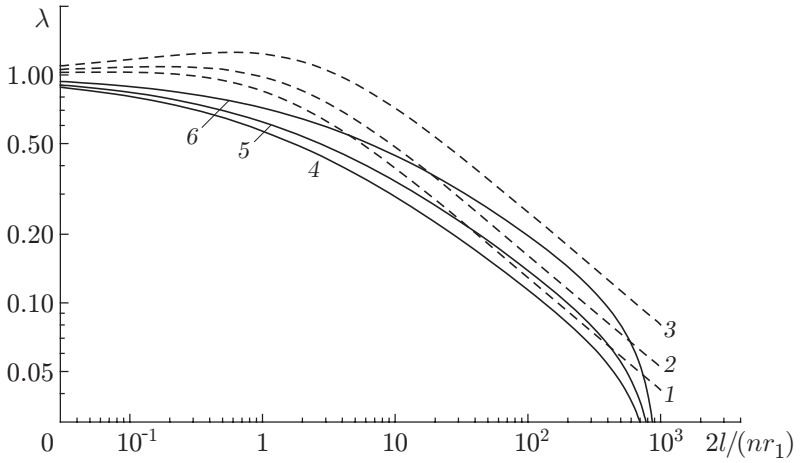

Fig. 2. Fracture diagrams of a square bimetallic plate with a central crack for $n = k = 1$, $c = 5/8$, and $\chi = 2.4$: (*1*) calculated by th formula (24) of the Kornev model; (*2*) calculated by formula (28) of the refined model corresponding to the minus sign; (*3*) calculated by formula (28); corresponding to the plus sign; (*4*) calculated by formula (13); (*5*) calculated by formula (21) corresponds to the minus sign; (*6*) calculated by formula (21) corresponding to the plus sign.

$$\Big[\lambda - \Big(\lambda\sqrt{1+\frac{nr_1}{2l}} - \frac{k}{n}\sqrt{\frac{nr_1}{2l}}\,\Big)\Big]\sqrt{\Delta} = \frac{\sqrt{2l}\,\chi c\lambda^2}{8}. \tag{26}$$

From (25) and (26), we express the critical length of the prefracture zone Δ and [using approximation (6)] the critical fracture stress λ as follows:

$$\Delta = \frac{\chi^2 c^2 \lambda^4 l^2}{16 nr_1}\Big[\frac{k}{n} - \lambda\Big(\sqrt{1+\frac{2l}{nr_1}} - \sqrt{\frac{2l}{nr_1}}\,\Big)\Big]^{-2}; \tag{27}$$

$$\lambda_{+,-} \approx \frac{k}{2n}\sqrt{\frac{nr_1}{2l}}\Big(2\sqrt{1+\frac{nr_1}{2l}} - 1 \pm \sqrt{1-\frac{2\chi c}{\pi}}\,\Big) \Big/ \Big(1+\frac{nr_1}{2l} - \sqrt{1+\frac{nr_1}{2l}} + \frac{\chi c}{2\pi}\Big). \tag{28}$$

Figure 2 shows fracture curves in double logarithmic coordinates for $n = k = 1$, $c = 5/8$, and $\chi = 2.4$. Calculations showed that for any plasticity index $0 < \chi \leqslant 4\pi/5$, curves *2 and 3* are located above curve *1*, i.e., the fracture load predicted by formula (28) is greater than the load predicted by formula (24) of the Kornev model. For $\chi = 0$, curve *2* coincides with curve *1*, and, hence, in this case there is a limiting transition from quasi-brittle to brittle fracture. For $\chi = 4\pi/5$, curve *2* coincides with curve *3*, and this value of χ is critical and corresponds to the transition point from the quasi-brittle fracture branch (λ_-) to the quasi-ductile fracture branch (λ_+). For the branch corresponding to quasi-ductile fracture (λ_+), the equality $\Delta_P \approx 30 r_{1P}$ is satisfied, which agrees well with the results of [12, p. 190], in which the approximate equality $\Delta \approx 34 r_1$ for the load $\lambda = 0.4$ was obtained for quasi-ductile fracture. Apparently, the inequality $\Delta < r_1$ is characteristic of quasi-brittle materials, and the inequality $\Delta > r_1$ for quasi-ductile materials. Note that in the coordinate system $(2l/(nr_1), \lambda)$, the position of curves *1–3* does not depend on the value of the parameter r_1.

Let us clarify the meaning of the parameter c, for which the single value $c = 5/8$ (plane stress state) was considered so far. In the case of a plane strain state, we have $c = (5 - 8\mu + 8\mu^2)/(8 - 8\mu^2)$, i. e., the parameter c characterizes the stress–strain state. At the same time, the value of c is proportional to the diameter a of the prefracture zone: $a = c\lambda^2 l$ [see (3), (16), and (26)]. The parameter c can be called a stiffness index or the reciprocal of the ductility index. The parameters c and χ are related: if $\chi c = \pi/2$, the branches corresponding to quasi-brittle (λ_-) and quasi-ductile (λ_+) fracture coincide, and if $c = 0$, formula (3) implies that $a = 0$ and, therefore, the equality $K_{\mathrm{I}\infty} + K_{\mathrm{I}\Delta} = 0$ of the Leonov–Panasyuk–Dugdale model holds. In the case $c = 0$, from Eq. (26) we obtain the following expression for the critical load:

$$\lambda = \frac{k}{n}\sqrt{\frac{nr_1}{2l}} \Big/ \Big(\sqrt{1+\frac{nr_1}{2l}} - 1\Big) = \frac{k}{n}\sqrt{\frac{2l}{nr_1}}\,\Big(\sqrt{1+\frac{nr_1}{2l}} + 1\Big),$$

which coincides with the expression for λ_+ in (28) for quasi-ductile fracture:

$$\lambda_+ \approx \frac{k}{2n}\sqrt{\frac{nr_1}{2l}}\left(2\sqrt{1+\frac{nr_1}{2l}}\right) \Big/ \left(1+\frac{nr_1}{2l}-\sqrt{1+\frac{nr_1}{2l}}\right) = \frac{k}{n}\sqrt{\frac{2l}{nr_1}}\left(\sqrt{1+\frac{nr_1}{2l}}+1\right).$$

In addition, for $c = 0$, Eq. (26) leads to the equality $\lambda = \lambda\sqrt{1+nr_1/(2l)} - k\sqrt{nr_1/(2l)}/n$, using which from Eq. (25) we obtain the expression $\lambda = 1 - 2\arcsin(1-\Delta/l)/\pi$, which relates the prefracture zone length to the load or $\Delta/l = 1 - \cos(\pi\lambda/2) \approx \pi^2\lambda^2/8 + 5\pi^4\lambda^4/384$. This expression is consistent with the expression $\Delta/l = \sec(\pi\lambda/2) - 1 \approx \pi^2\lambda^2/8 - \pi^4\lambda^4/384$ given in [13, p. 65] for the Leonov–Panasyuk–Dugdale model.

Similarly calculations are carried out if the normal stresses $\sigma_y(x,0)$ are represented by relation (9), which takes into account the finite dimensions of the plate. Then, for $c = 0$ [hence, according to Eq. (16), $K_{\mathrm{I}\infty} + K_{\mathrm{I}\Delta} = 0$] from Eq. (18) we express the critical load as $\lambda = k(L-2l)/L/n$, which coincides with expression (21) for λ_+ for quasi-ductile fracture. Equation (17) leads to the equality $\lambda Y/\sqrt{\pi} = 1 - 2\arcsin(1-\Delta/l)/\pi$, from which, using the relation $Y = \sqrt{\pi/\cos(\pi l/L)}$, we express the length of the pre-fracture zone as $\Delta/l = 1 - \cos(\pi\lambda/(2\sqrt{\cos(\pi l/L)}))$. For small crack lengths ($l/L \ll 1$), this expression is consistent with the expression for the length Δ in the Leonov–Panasyuk–Dugdale model.

Figure 2 also shows fracture curves *4–6* constructed for $r_1 = 0.118$ by formulas (13) and (21), taking into account the finite dimensions of the bimetallic plate. In the coordinate system $(2l/(nr_1), \lambda)$, curves *4–6* depend on the parameter r_1, but for any value of r_1, curves *4, 5, and 6* lie below curves *1, 2, and 3*, respectively.

3.3. Fracture Diagrams of a Homogenous Structured Material

Results of a finite element simulation of crack propagation in a homogeneous material are presented in [12]. As in [12], we substitute into equality (1) the representation of the normal stress $\sigma_y(x,0)$ on the crack continuation due to the stress σ_∞:

$$\sigma_y(x,0) \approx \frac{K_{\mathrm{I}\infty}}{\sqrt{2\pi x}} + \sigma_\infty + \frac{K_{\mathrm{I}\Delta}}{\sqrt{2\pi x}}, \qquad K_{\mathrm{I}\infty} = \sigma_\infty\sqrt{\pi l}. \tag{29}$$

For the diameter of the prefracture zone in the homogeneous material in a plane stress state, we will use the expression $a = 5\lambda^2 l/4$, which differs from expression (3). Performing the procedure described in Section 2, for the refined analytical model we obtain the following system of approximate equations for the length Δ of the prefracture zone and the dimensionless critical load λ:

$$\Delta = \frac{25\chi^2}{2^{11}}\lambda^2 l\,\frac{2l}{nr_1}\Big(\frac{k}{n\lambda}-1\Big)^{-2}; \tag{30}$$

$$\lambda = \frac{k}{n}\Big(2+\sqrt{\frac{2l}{nr_1}}\left(1\pm\sqrt{1-\frac{5\chi}{2\pi}}\right)\Big) \Big/ \Big(2+2\sqrt{\frac{2l}{nr_1}}+\frac{5\chi}{4\pi}\,\frac{2l}{nr_1}\Big). \tag{31}$$

Figure 3 shows fracture curves for the homogeneous material. Curve *1* is constructed by the formula

$$\lambda = 1/(1+\sqrt{2l/r_1}\,), \tag{32}$$

which, for $\chi = 0$ (brittle fracture), corresponds to representation (29) of the normal stress on the crack continuation in the Kornev model. As in [12], curve *1* is obtained for $r_1 = 0.118$.

Curve *2* is constructed by the formula

$$\lambda = 1/\sqrt{0.9999 + 16.95l}\,, \tag{33}$$

which was chosen as a result of a least-squares approximation of numerical simulation results [12]. FEM numerical simulation was performed for a square steel plate of size $100.0 \times 100.0 \times 0.4$ mm. The length $2l$ of the internal crack was varied from 4 to 90 mm. Curve *3* was constructed by formula (31) of the refined model for $\chi = 0.0001$ and $n = k = 1$. Formula (31) contains the plus sign before the square root. The value of the parameter r_1 was chosen so as to match the load values λ calculated by formulas (31) and (33) for $l = 2$. It is evident in Fig. 3 that at small crack length ($l < 5$), curve *2* is better approximated by curve *3* than by curve *1*. The deviation of curve *3* for $l > 5$ is due to the influence of the finite dimensions of the plate, which was neglected in model (30), (31).

To account for the finite dimensions of the homogeneous square plate, we represent the normal stresses $\sigma_y(x,0)$ on the central crack continuation in the form (9), and express the diameter of the prefracture

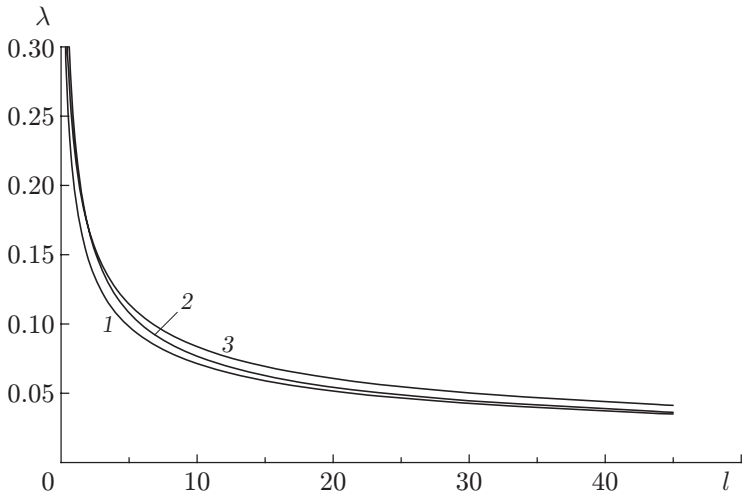

Fig. 3. Fracture curves for the homogeneous material: (*1*) calculated by formula (32); (*2*) calculated by formula (33); (*3*) calculated by formula (31).

zone in the homogeneous material in a plane stress state as $a = 5\lambda^2 l/4$. Then, for the Kornev model, we have the following system of equations for the length of the prefracture zone Δ and the dimensionless critical load λ:

$$\Delta = 25\chi^2\lambda^2 l Y^2/(2^9\pi); \tag{34}$$

$$\lambda = \frac{k}{n}\Big[\frac{Y}{\sqrt{\pi}}\sqrt{\frac{2l}{nr_1}}\Big(1-\frac{5\chi}{8\pi}\Big)+\frac{L}{L-2l}\Big]^{-1}, \tag{35}$$

and for the refined model, the system of equations

$$\sqrt{\Delta} = \frac{5\chi Y^2}{16\pi}\lambda^2 l\Big[\Big(\frac{k}{n}-\frac{L\lambda}{L-2l}\Big)\sqrt{nr_1}\,\Big]^{-1}; \tag{36}$$

$$\lambda_{1,2} = \frac{k}{n}\Big(\frac{2L}{L-2l}+\frac{Y}{\sqrt{\pi}}\sqrt{\frac{2l}{nr_1}}\,\Big(1\pm\sqrt{1-\frac{5\chi}{2\pi}}\,\Big)\Big)\Big/\Big(\frac{2L^2}{(L-2l)^2}+\frac{2LY}{L-2l}\sqrt{\frac{2l}{\pi nr_1}}+\frac{5\chi Y^2 l}{2\pi^2 nr_1}\Big). \tag{37}$$

Relations (34), (35), and (36), (37) differ from relations (12), (13) and (19), (21), respectively, in numerical coefficients: in the bimaterial ($c = 5/8$), the diameter a of the prefracture zone is half that in the homogeneous material ($c = 5/4$).

Figure 4 shows fracture curves for the homogeneous square plate. Curve *1* is constructed using formula (35) which, for $\chi = 0$ (brittle fracture) corresponds to representation (9) of the normal stress on the crack continuation in the Kornev model. As in [12], curve *1* is constructed for $r_1 = 0.118$. Curve *2* is constructed by formula (33), and curve *3* by formula (37) of the refined model for $\chi = 0.0001$ and $n = k = 1$. In formula (37), the plus sign before the square root was used (quasi-ductile fracture). The value of the parameter r_1 was chosen so as to match the load values λ calculated by formulas (37) and (33) for $l = 2$. Comparison of the curves given in Figs. 3 and 4 with the results of [12] shows that curve *3* in Fig. 4 is better consistent with the results of the numerical experiment.

4. DISCUSSION OF THE SIMULATION RESULTS

In the present work, we obtained the exact expression (19) for the length of the prefracture zone of quasi-brittle materials in the Kornev model. This expression was used to refine expression (21) for the critical fracture load. Analysis of relations (14) and (21) showed that the range of admissible values of the parameter χ in the refined Kornev model is four times smaller than the range of admissible values of χ corresponding to the simplified relation (13) in the Kornev model.

Introduction of the new parameter c to this model made it possible to supplement the model with formulas for the length of the prefracture zone and the critical load for quasi-ductile fracture of materials. The comparison

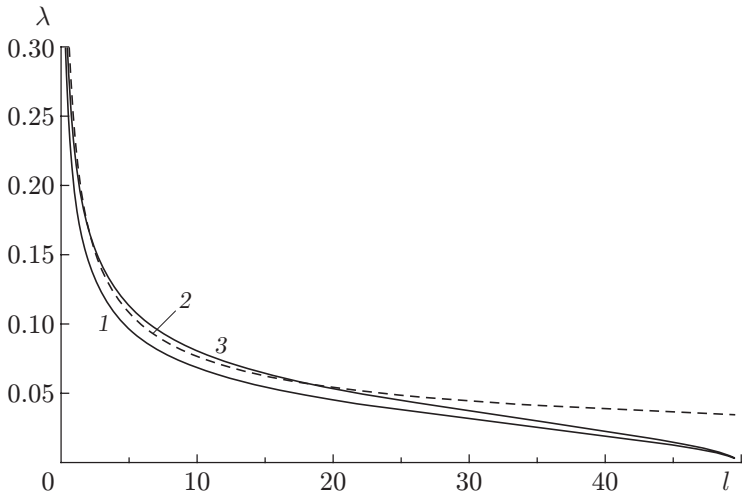

Fig. 4. Fracture curves for the square metal plate: (*1*) calculated by formula (35); (*2*) calculated by formula (33); (*3*) calculated by formula (37).

made in Section 3 showed good agreement between the results of FEM simulations [10, 12] and the theoretical estimates obtained using the refined model presented in this paper in the case of quasi-ductile fracture.

In [11], the fracture of a laminated composite was studied within the framework of the Kornev models using formulas for the critical loads taking into account the finite dimensions of the samples. However, processing of the results of full-scale experiments using the Kornev model for quasi-brittle materials involved difficulties: it was often not possible to find a numerical solution of the constitutive equations. Perhaps these difficulties are partly due to restriction on the parameter $\chi \leqslant 2.5$, which in [11] was not always satisfied.

5. CONCLUSIONS

In this paper, refined formulas for the critical length of the prefracture zone and the critical load for quasi-brittle materials were proposed. The Kornev model was extended to the case of quasi-ductile materials.

When using the analytical model to describe the fracture of structured materials, the geometry of the samples and the mechanical characteristics of the sample materials are taken into account, in particular, the parameter characterizing the linear size of the structural element of the material.

Analysis of the calculation results suggests that the Kornev model provides a qualitative estimate of the fracture load depending on the length of the initial crack. Thus, the analytical model considered here can be used to study the deformation and fracture of composites of structured materials. This will allow a reduction in the amount of full-scale tests required to evaluate the fracture load.

This work was supported by the Russian Foundation for Basic Research (Grant No. 14-08-00113) and the Program for Basic Studies of Russian Academy of Sciences (No. 01201365412).

REFERENCES

1. N. Eaton, A. Glover, and J. McGrath, "Features of Fracture in the Manufacture and Operation of Welded Structures," in *Fracture Mechanics. Fracture of Structures* (Mir, Moscow, 1980), Issue 20, pp. 92–120.
2. D. M. Lipkin, G. E. Beltz, and D. R. Clarke, "A Model of Cleavage Fracture along Metal/Ceramic Interfaces," Mater. Res. Soc. Symp. Proc. **436**, 91–96 (1997).
3. D. Broek, *Elementary Engineering Fracture Mechanics* (Springer, 1982).
4. S. V. Suknev, "The Use of Nonlocal and Gradient Criteria to Evaluate the Fracture of Geomaterials in Regions of Tensile Stress Concentration," Fiz. Mezomekh. **14** (2), 67–75 (2011).

5. S. Usami, H. Kimoto, I. Takanashi, and S. Shida, "Strength of Ceramic Materials Containing Small Flaws," Eng. Fract. Mech. **23** (4), 745–761 (1986).
6. Yun-Jae Kim and Karl-Heinz Schwalbe, "Mismatch Effect on Plastic Yield Loads in Idealised Weldments. 2. Heat Affected Zone Cracks," Eng. Fract. Mech. **68**, 183–199 (2001).
7. V. M. Kornev, "Generalized Sufficient Strength Criteria. Description of the Prefracture Zone," Prikl. Mekh. Tekh. Fiz. **43** (5), 153–161 (2002) [J. Appl. Mech. Tech. Phys. **43** (5), 763–769 (2002)].
8. V. M. Kornev, "Stress Distribution and Crack Opening in the Prefracture Zone (Neuber–Novozhilov Approach)," Fiz. Mezomekh. **7** (3), 53–62 (2004).
9. V. M. Kornev and N. S. Astapov, "Model of the Fracture of a Piecewise Homogeneous Medium for Layering of Elastoplastic Structured Materials," Mekh. Kompoz. Mater. Konstr. **16** (3), 347–360 (2010).
10. V. D. Kurguzov, V. M. Kornev, and N. S. Astapov, "Fracture Model for Bimaterials in Layering. Numerical Experiment," Mekh. Kompoz. Mater. Konstr. **17** (4), 462–473 (2011).
11. A. G. Demeshkin, V. M. Kornev, and N. S. Astapov, "Strength of a Laminated Composite in the Presence of Crack-Like Defects," Mekh. Kompoz. Mater. Konstr. **19** (3), 445–458 (2013).
12. V. D. Kurguzov and V. M. Kornev, "Construction of Quasi-Brittle and Quasi-Ductile Fracture Diagrams Based on Necessary and Sufficient Criteria," Prikl. Mekh. Tekh. Fiz. **54** (1), 179–194 (2013) [J. Appl. Mech. Tech. Phys. **54** (1), 156–169 (2013)].
13. I. M. Kershtein, V. D. Klyushnikov, E. V. Lomakin, and S. A. Shesterikov, *Based on Experimental Fracture Mechanics* (Moscow State Univ., Moscow, 1989) [in Russian].
14. V. M. Kornev and A. G. Demeshkin, "Quasi-Brittle Fracture Diagram of Structured Bodies in the Presence of Edge Cracks," Prikl. Mekh. Tekh. Fiz. **52** (6), 152–164 (2011) [J. Appl. Mech. Tech. Phys. **52** (6), 975–985 (2011)].
15. Yu. G. Yanovskii, *Nanomechanics and Strength of Composite Materials* (Institute of Applied Mechanics of the Russian Academy of Sciences, Moscow, 2008) [in Russian].